Molecular Crystals and Liquid Crystals

Publication details, including instructions for authors and subscription information:
http://www.tandfonline.com/loi/gmcl20

Relationship between Film Structure and Electric Performance of Organic Field-Effect Transistors Based on Perylene Tetracarboxylic Diimide Derivatives

Yoshinobu Hosoi [a] & Yukio Furukawa [a]

[a] Department of Chemistry, School of Science and Engineering, Waseda University, Shinjuku-ku, Tokyo, Japan

Version of record first published: 22 Sep 2010

To cite this article: Yoshinobu Hosoi & Yukio Furukawa (2007): Relationship between Film Structure and Electric Performance of Organic Field-Effect Transistors Based on Perylene Tetracarboxylic Diimide Derivatives, Molecular Crystals and Liquid Crystals, 471:1, 189-194

To link to this article: http://dx.doi.org/10.1080/15421400701548191

Mol. Cryst. Liq. Cryst., Vol. 471, pp. 189–194, 2007

ISSN: 1542-1406 print/1563-5287 online
DOI: 10.1080/15421400701548191

Relationship between Film Structure and Electric Performance of Organic Field-Effect Transistors Based on Perylene Tetracarboxylic Diimide Derivatives

Yoshinobu Hosoi
Yukio Furukawa
Department of Chemistry, School of Science and Engineering, Waseda University, Shinjuku-ku, Tokyo, Japan

We have fabricated organic field-effect transistors (OFETs) based on three derivatives of perylene tetracarboxylic diimide (PTCDI). The electron mobility more than $8 \times 10^{-2}\,cm^2V^{-1}s^{-1}$ has been obtained in both vacuum and air for N,N′-bis(4-fluorobenzyl)perylene-3,4,9,10-tetracarboxylic diimide. The study of the film structures suggests that the flat-layer structures near the SiO_2 surfaces induce the high electron mobilities.

Keywords: atomic force microscopy; infrared spectroscopy; organic field-effect transistor; perylene tetracarboxylic diimide

INTRODUCTION

High performance n-channel organic field-effect transistors (OFETs) are crucial components for making bipolar transistors and complementary circuits [1]. Perylene tetracarboxylic diimide (PTCDI) derivatives are promising candidates for active layers in n-channel OFETs. In particular, the derivatives with alkyl chains as *N*-substituents show the highest electron mobilities more than $1\,cm^2V^{-1}s^{-1}$ [2–6]. In the present study, we have fabricated the n-channel OFETs based on three PTCDI derivatives with different *N*-substituents, *N*,*N*′-bis(4-fluorobenzyl)perylene-3,4,9,10-tetracarboxylic diimide (PTCDI-PFB), *N*,*N*′-bis(octyl)perylene-3,4,9,10-tetracarboxylic diimide (PTCDI-C_8),

This work was supported by a Grant-in-Aid for Young Scientists (B) (18750170) from JSPS and the 21COE "Practical Nano-Chemistry" from MEXT.

Address correspondence to Yoshinobu Hosoi, Department of Chemistry, School of Science and Engineering, Waseda University, Shinjuku, Tokyo 169-8555, Japan. E-mail: hosoi@aoni.waseda.jp

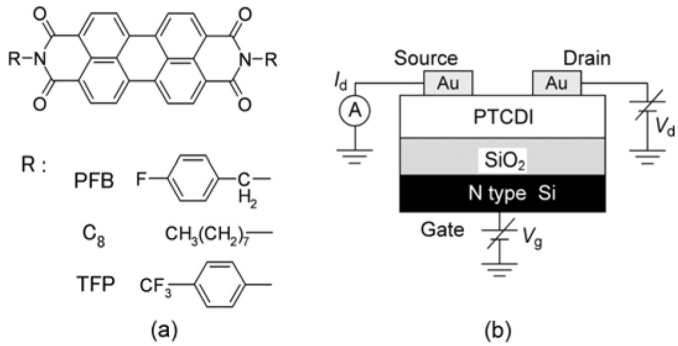

FIGURE 1 (a) Chemical structures of PTCDI derivatives. (b) Schematic device structure of an OFET based on a PTCDI derivative.

and *N*,*N*′-bis(4-trifluoromethylphenyl)perylene-3,4,9,10-tetracarboxylic diimide (PTCDI-TFP), as shown in Figure 1a. Figure 1b shows the schematic structure of the top-contact OFETs prepared in this study. Our study focuses on the morphology and the molecular orientation of the PTCDI derivatives in the films, because the solid-state structure close to the SiO_2 surface of an OFET deeply affects the performance of the device. Atomic force microscopy (AFM) and infrared spectroscopy have been used for the analysis of the film structures.

EXPERIMENTAL

A highly doped n-type silicon wafer (0.02 Ωcm, ⟨100⟩ axis) covered with a thermally grown SiO_2 layer (thickness, ca. 500 nm) was purchased from Sansho Shoji Co. Ltd. A substrate was immersed in a 1:1 mixture of concentrated H_2SO_4 and H_2O_2 (30% water solution) for 10 min. The cleaned substrate was kept in a Teflon® container including neat hexamethyldisilazane (HMDS) at room temperature for more than 12 h. The PTCDI derivatives were synthesized according to the previous method [7] and purified by vacuum sublimation. The 40-nm thick film of each derivative was prepared by vacuum vapor deposition at a rate of 0.5–1.0 nm/min at various substrate temperatures (T_s). Top-contact interdigital source and drain electrodes were made with gold through a shadow mask by vacuum vapor deposition. The length (L) and width (W) of the channel were 50 μm and 60 mm, respectively.

Electrical characteristics of OFETs were measured at a pressure below 1×10^{-1} Pa using two Keithley Model 6487 picoammeter/voltage oltage source units. AFM and infrared measurements were performed

for the thin films prepared on an n-type silicon substrate (1-5 Ωcm, ⟨100⟩ axis) covered with a thermally grown SiO_2 layer (thickness, ca. 500 nm) purchased from Sansho Shoji Co. Ltd, which can transmit infrared light. The substrates and films were prepared in the same manner as the OFETs described above were made. Tapping-mode AFM images were recorded on a Digital Instruments Dimension 3100 AFM. Infrared spectra of the films were measured in a transmission-absorption configuration on a Varian FTS-7000e FT-IR spectrometer equipped with a linearized HgCdTe detector.

RESULTS AND DISCUSSION

Figure 2a shows the output characteristics of the OFET based on PTCDI-PFB at $T_s = 100^{\circ}C$. The OFET behaves in the n-channel and accumulation mode. The filled circles in Figure 2b show the transfer characteristics at the saturation region for the OFET measured in vacuum. An electron mobility (μ_e) and a threshold voltage (V_{th}) at the saturation region were derived in a standard manner by the following Eq. (8):

$$I_{d,sat} = \frac{W\mu_e C}{2L}(V_g - V_{th})^2 \tag{1}$$

where $I_{d,sat}$, C, and V_g are the drain current at the saturation region, the capacitance per unit area of the SiO_2 gate dielectric, and the gate voltage, respectively. We have defined the on/off ratio as the ratio of I_d between $V_g = 100$ V and $V_g = -50$ V. The calculated electron mobility, threshold voltage, and on/off ratio are $8.8 \times 10^{-2}\,cm^2\,V^{-1}\,s^{-1}$, 24 V, and 10^6, respectively. The transfer characteristics measured after

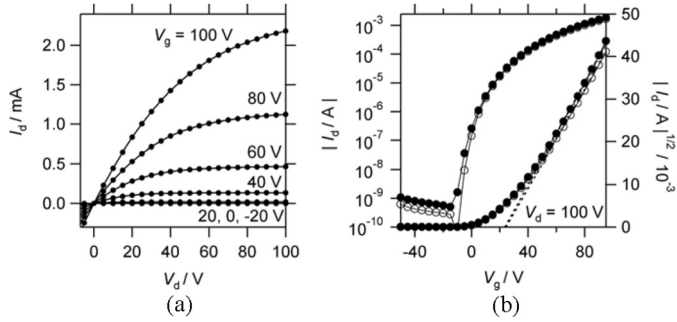

FIGURE 2 (a) Output characteristics for the PTCDI-PFB OFET. (b) Transfer characteristics for the PTCDI-PFB OFET. The filled and open circles show the drain current in vacuum and in air, respectively.

TABLE 1 Electron Mobilities Calculated from Eq. (1) on the n-Channel OFETs Based on PTCDI Derivatives

	T_s/°C	μ_e/cm^{2}V^{-1}s^{-1}
PTCDI-PFB	100	8.8×10^{-2}
PTCDI-C_8	80	4.9×10^{-1}
PTCDI-TFP	115	4.0×10^{-4}

air-exposure for 30 minutes are shown with the open circles in Figure 2b. The open circles mostly coincide with the filled, indicating that the OFET based on PTCDI-PFB can operate stably in air without degradation. The calculated electron mobility, threshold voltage, and on/off ratio in air are $8.2 \times 10^{-2}\,cm^2\,V^{-1}\,s^{-1}$, 25 V, and 10^6, respectively.

Table 1 shows the highest mobility of each PTCDI derivative measured in vacuum and T_s. The mobilities strongly depend on the *N*-substituents. PTCDI-C_8 shows relatively a high electron mobility, as reported in previous papers [2,3]. On the other hand, the OFET based on PTCDI-TFP has a very low mobility.

Figure 3 shows the infrared spectra of the PTCDI-PFB films on the HMDS-treated SiO_2 substrates at $T_s = 100°C$. The bands observed at 1693, 1656 and 812 cm^{-1} are called the *X*, *Y*, and *Z* modes, respectively.

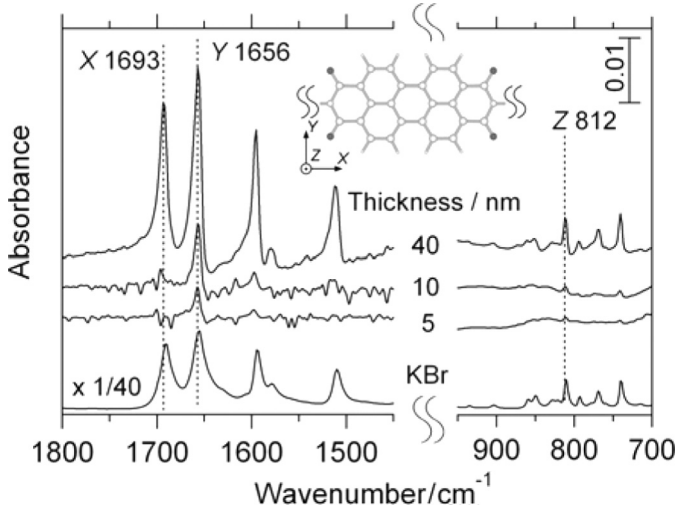

FIGURE 3 Infrared spectra for 5-, 10-, and 40-nm films of PTCDI-PFB. The bottom curve shows the spectrum of randomly oriented crystals of PTCDI-PFB in a KBr disk.

The *X* and *Y* modes are assigned to the symmetric and antisymmetric stretching vibrations of C=O in the imide groups, respectively. The *Z* mode is assigned to the CH out-of-plane bending in the perylene ring. These modes have the transition dipole moments parallel to the *X*, *Y*, and *Z* axes in the inset of Figure 3, respectively. In the 40-nm film, the *X* mode is observed strongly, whereas the intensity of the *X* mode becomes remarkably weak in the 5- and 10-nm films. In the transmission configuration, vibrational modes whose transition dipole components are parallel to the substrate are enhanced, and while those perpendicular to the substrate are suppressed. Thus, the dipole moment of the *X* mode is perpendicular to the substrate. In other words, the PTCDI-PFB molecules are arranged with their perylene skeletal planes nearly perpendicular to the surface. The molecular orientation depends on the film thickness.

The molecular orientations of PTCDI-C_8 and -TFP have also been evaluated by infrared spectroscopy. In the PTCDI-C_8 film, perylene skeletal planes are nearly perpendicular to the surface in the 5- to 40-nm thick film. On the other hand, perylene planes are randomly oriented in the PTCDI-TFP film.

The AFM images of the PTCDI-PFB films are shown in Figures 4a–d. The 1.2-nm film exhibits many small grains with the sizes from 100 to 200 nm (Fig. 4a). As the thickness increases, the grains grow along the substrate surface and coalesce with the neighboring grains. The 2.5-nm film indicates that the substrate is almost covered with the first monolayer (Fig. 4b). The morphology of the 10-nm film in

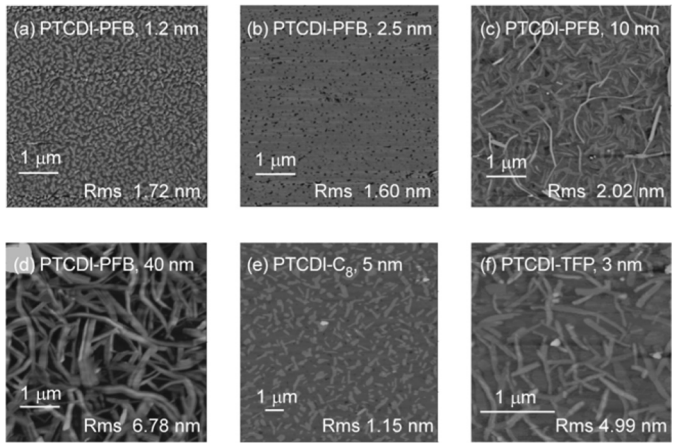

FIGURE 4 AFM images of (a–d) PTCDI-PFB films, (e) a PTCDI-C_8 film, and (f) a 3-nm PTCDI-TFP film.

Figure 4c indicates the successive formation of the flat layers in the growth process similar to the first monolayer. The root-mean-square roughnesses (R_{ms}) are as small as 1.5–2.0 nm in the region of the thicknesses less than 10 nm. However, a few fiber-like grains are observed in the 10-nm film. With the further film growth, a rough surface with only fiber-like grains appears in the 40-nm film as shown in Figure 4d.

Figures 4e, f show the AFM images of the 5-nm film of PTCDI-C_8 and the 3-nm film of PTCDI-TFP films. The PTCDI-C_8 film has a very smooth surface with a flat-layer structure. Probably, a flat-layer structure close to the SiO_2 surface plays an important role for the high electron mobilities with OFETs based on PTCDI-PFB and PTCDI-C_8. On the other hand, the fiber-like grains appear in the PTCDI-TFP film, even close to the substrate surface. The fiber-like grains may inhibit transportation of charge carriers due to many grain boundaries.

SUMMARY

The OFET based on the PTCDI-PFB film has demonstrated a high electron mobility and air-stability. PTCDI-PFB and PTCDI-C_8 molecules close to the HMDS modified SiO_2 surfaces are arranged with their perylene skeletal planes perpendicular to the substrates. These films consist of the large flat-layer structures, which induce the high electron mobilities. On the other hand, the PTCDI-TFP film, which provides the low mobility, consists of the fiber-like grains.

REFERENCES

[1] Newman, C. R., Frisbie, C. D., da Silva Filho, D. A., Brédas, J.-L., Ewbank, P. C., & Mann, K. R. (2004). *Chem. Mater.*, *16*, 4436.
[2] Malenfant, P. R. L., Dimitrakopoulos, C. D., Gelorme, J. D., Kosbar, L. L., Graham, T. O., Curioni, A., & Andreoni, W. (2002). *Appl. Phys. Lett.*, *80*, 2517.
[3] Chesterfield, R. J., McKeen, J. C., Newman, C. R., Frisbie, C. D., Ewbank, P. C., Mann, K. R., & Miller, L. L. (2004). *J. Appl. Phys.*, *95*, 6396.
[4] Chesterfield, R. J., McKeen, J. C., Newman, C. R., Ewbank, P. C., Filho, D. A. S., Brédas, J. L., Miller, L. L., Mann, K. R., & Frisbie, C. D. (2004). *J. Phys. Chem. B*, *108*, 19281.
[5] Unni, K. N. N., Pandey, A. K., & Nunzi, J. M. (2005). *Chem. Phys. Lett.*, *407*, 95.
[6] Gundlach, D. J., Pernstich, K. P., Wilckens, G., Gruter, M., Haas, S., & Batlogg, B. (2005). *J. Appl. Phys.*, *98*, 064502.
[7] Demmig, S. & Langhals, H. (1988). *Chem. Ber.*, *121*, 225.
[8] Sze, S. M. (1981). *Physics of Semiconductor Devices*, 2nd ed., Wiley-Interscience: New York, 374.